No-sticking effect and quantum reflection in ultracold collisions

Areez Mody, Michael Haggerty, John M. Doyle, and Eric J. Heller
Department of Physics, Harvard University, Cambridge, Massachusetts 02138
and Center for Ultracold Atoms, Harvard University and MIT, Cambridge, Massachusetts 02138
(Received 20 October 2000; revised manuscript received 4 May 2001; published 8 August 2001)

We provide a general and nonperturbative theoretical basis for quantum reflection of an ultracold atom incident on a cold or warm surface. Sticking is identified with the formation of a long-lived resonance, from which it emerges that the physical reason for not sticking is that the many internal degrees of freedom of the target serve to decohere the incident one body wave function, thereby upsetting the delicate interference process necessary to form a resonance. We then explore the transition to the post-threshold behavior, when sticking prevails at higher incident energies. Studying the WKB wave functions of the atom provides a quick understanding of our results even in the ultracold regime where WKB is not applicable. Explicit examples are examined in detail and we predict the temperatures required to reach the various regimes.

DOI: 10.1103/PhysRevB.64.085418 PACS number(s): 34.10.+x, 34.50.−s

I. INTRODUCTION

The problem of low-energy sticking to surfaces has attracted much attention over the years.[1–5] The controversial question has been the ultralow energy limit of the incoming species, for either warm or cold surfaces. A battle has ensued between two countervailing effects, which we will call classical sticking and quantum reflection. The concept of quantum reflection is intimately connected with threshold laws, and was recognized in the 1930s by Lennard-Jones.[1] Essentially, flux is reflected from a purely attractive potential with a probability which goes as $1-\alpha\sqrt{\epsilon}$, as $\epsilon\to 0$, where α is a constant and ϵ is the translational energy of the particle incident on the surface. Classically the transmission probability is unity. Reflection at long range prevents inelastic processes from occurring, but if the incoming particle should penetrate into the strongly attractive region, the ensuing acceleration and hard collision with the repulsive short-range part of the potential leads to a high probability of inelastic processes and sticking.

If the WKB approximation were correct everywhere, sticking would be the rule, since WKB is based on the classical motion which leads to sticking at low incident energies. The blame for the quantum reflection can thus be laid at the feet of the WKB approximation, which breaks down in the long-range attractive part of the potential at low energy. Very far out, the WKB is good even for low energy, because the potential is so nearly flat. Close in, the kinetic energy is high, because of the attractive potential, even if the asymptotic energy is very low, and again WKB is accurate. But in between there is a breakdown, which has been recognized and exploited by several groups.[6–11,20] We show that this breakdown occurs in a region around $|V|\approx\epsilon$; i.e., approximately where the kinetic and potential energies are equal.

It would seem that quantum reflection would settle the issues of sticking, since if the particle does not make it in close to the surface there is no sticking (Fig. 1). There is one caveat, however, which must be considered: quantum reflection can be defeated by the existence of a resonance in the internal region, i.e., a threshold resonance (Fig. 2).

The situation is very analogous to a high-Q Fabry-Perot cavity, where using nearly 100% reflective, parallel mirrors gives near 100% reflection except at very specific wavelengths. At these specific energies a resonace buildup occurs in the interior of the cavity, permitting near 100% transmission. Such resonances are rare in a one-dimensional world, but the huge number of degrees of freedom in a macroscopic solid particle makes resonances ubiquitous. Indeed, the act of colliding with the surface, creating a phonon, and dropping into a local bound state of the attractive potential describes a Feshbach resonance. Thus the resonances are just the sticking we are investigating, and we must not treat them lightly! Perhaps it is not obvious after all whether sticking occurs.

After the considerable burst of activity surrounding the sticking issue on the surface of liquid helium,[12,13,23] and after a very well executed theoretical study by Clougherty and Kohn,[4] the controversy has settled down, and the common wisdom has grown that sticking does not occur at sufficiently low energy. While we agree with this conclusion, we believe the theoretical foundation for it is not complete, nor stated in a wide enough domain of physical situations. For example, Ref. 4 treats only a harmonic slab with one or two phonon excitation. It is not clear whether the results apply to a warm surface. On the experimental side, even though quantum reflection was observed from a liquid-helium surface, that surface has a very low density of available states (essentially only the ripplons) which could be a special case with respect to sticking. Thus the need for more rigorous and clear proof of nonsticking in general circumstances is evident. This paper gives such an analysis.

The strategy we use puts a very general and exact scattering formalism to work, providing a template into which to insert the properties of our target and scatterer. Then very general results emerge, such as the nonsticking theorem at zero energy. The usual procedure of defining model potentials and considering one phonon processes, etc., is not necessary. All such model potentials and Hamiltonians wind up as parameters in the R-matrix formalism. The details of a particular potential are of course important for quantitative results, but the range of possible results can be much more easily examined by inserting various parameters into the R-matrix formalism. All the possible choices of R-matrix parameters give the correct threshold laws. Certain trends are built into the R-matrix formalism which are essentially inde-

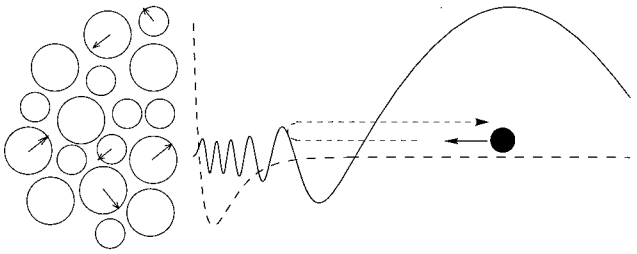

FIG. 1. The stationary state one body wave function of the incident atom moving in the mean potential felt by it. The amplitude inside the interaction region is supressed by $k_e \sim \sqrt{\epsilon}$. This is tantamount to the reflection of the atom.

pendent of the details of the potentials. Indeed, it was this fact that allowed Wigner to derive some scattering threshold laws, using *R*-matrix theory.

Having established the ineffectiveness of the resonances and the essential correctness of the simplistic one body physics of quantum reflection (Sec. III) from the surface, we move on in the second half of the paper to predict the quantitative sticking probabilities for different surface-atom pairs. From an experimental perspective, atom-surface sticking could impact the area of guiding and trapping atoms in material wires and containers. In those applications it is necessary to predict the velocities needed for quantum reflection, sticking, and the transition regime between them. The reader interested mainly in practical results may safely start reading from Sec. IX onwards, after glancing only at Sec. III in which we briefly consider the problem perturbatively in order to better elucidate the role played by quantum reflection. We emphasize that none of the perturbation section is actually necessary for our final conclusions.

II. GEOMETRY AND NOTATION

The incident atom is treated as a point particle at position (x,y). To keep the notation simple we leave out the z coordinate and confine our discussion to two spatial dimensions. Thus a cross section will have dimensions of length, etc. It will be quite obvious how and where z may be inserted in all that follows. Let u represent all the bound degrees of freedom of the scattering target, which we take to be a slab of crystalline or amorphous material. Let $\Omega_c(u)$, $c=1,2,\ldots,$ be the many-body target wave functions in the absence of interactions with the incident particle, and having energy

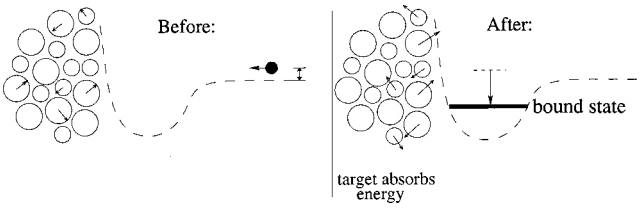

FIG. 2. A schematic view of a Feshbach resonance wherein the incident atom forms a long-lived quasibound state with the target. The many-body wave function in this situation (not shown) has a large amplitude in the ''interior'' region near the slab.

E_c^{target}. These are normalized as $\int_{\text{all u}} du |\Omega_c(u)|^2 = 1$. x is the distance of the scatterer (atom) from the face of the slab which is approximately (because the wall is rough) along the line $x=0$. The internal constituents of the slab lie to the left of $x=0$ and the scatterer is incident from the right with kinetic energy $\epsilon = \hbar^2 k_e^2/2m$. The total energy E of the system is

$$E = \epsilon + E_e^{\text{target}}, \tag{1}$$

where $c=e$ is the index of the ''entrance channel'' i.e., the initial internal state of the slab before the collision is $\Omega_e(u)$. Notice that we say nothing about the value of E_e^{target} itself. In particular the slab need not be cold. k_c is the magnitude of the wave vector $\vec{k}_c$ of the particle when it leaves the target in the state $\Omega_c(u)$ after the collision. Our interest focusses on $k_e \to 0$. k_e is the magnitude of the wave vector of the incoming particle. For the open channels $c=1,\ldots n$ (this defines n) for which $E > E_c^{\text{target}}$, $k_c \equiv \sqrt{2m(E-E_c^{\text{target}})/\hbar^2}$ $(c \leqslant n)$; whereas for the closed channels $(c>n)$, $E < E_c^{\text{target}}$, and $k_c \equiv i\sqrt{2m(E_c^{\text{target}}-E)/\hbar^2} \equiv i\kappa_c$ $(c>n)$. $\kappa_c > 0$. We will use (k_{cx}, k_{cy}) as the x,y components of $\vec{k}_c$. Let $U^{(\text{int})}(x,y,u) = (2m/\hbar^2) V^{(\text{int})}(x,y,u)$, where $V^{(\text{int})}(x,y,u)$ describes quite generally the interaction potential between the incident atom and all the internal degrees of freedom of the slab. For simplicity we assume for the moment that there is no interaction between slab and atom for $x > a$.

III. PRELIMINARIES: PERTURBATION

As stated above, we excercise the perturbative treatment for insight only; our final conclusions are based on nonperturbative arguments. We treat the interaction $U^{(\text{int})}(x,y,u)$ between slab and atom by separating out a ''mean'' potential felt by the atom that is independent of y and u; call it $U^{(0)}(x)$, and treat the remainder $U^{(1)}(x,y,u) \equiv U^{(\text{int})}(x,y,u) - U^{(0)}(x)$ as a perturbation.

Now the incident beam is scattered by the entire length (say from $y=-L$ to $L=2L$) of wall which it illuminates. If all measurements are made close to the wall so that its length $2L$ is the largest scale in the problem, then it is appropriate to speak of a cross section per unit length of wall, a dimensionless probability. More specifically, we will assume that the matrix elements $U^{(1)}_{cc'}(x,y) \equiv \int_{\text{all u}} du \Omega_c^*(u) U^{(1)}(x,y,u) \Omega_{c'}(u)$ of the perturbation $U^{(1)}(x,y,u)$ are given by the simple form $U^{(1)}_{cc'}(x,y) = U^{(1)}_{cc'}(x) f(y)$ for $y \in [-L,L]$ and 0 elsewhere. $f(y)$ is a random persistent (does not die to 0 as $|L| \to \infty$) function that models the random roughness of the slab and is characterized by its so-called spectral density function S, a smooth positive-valued nonrandom function, such that

$$\left| \int_{-L}^{L} dy e^{iky} f(y) \right|^2 \equiv 2L\ S(k) \tag{2}$$

as $L \to \infty$.

Now, applying either time-independent perturbation (equivalently the Born approximation for this geometry) or

time-dependent perturbation theory via the Golden Rule, we find that the cross section per unit length of wall for inelastic scattering to a final channel c is

$$P^{\rm in}_{c\leftarrow e}(\theta)=\frac{2\pi}{k_e}\left(\int_{-\infty}^{a}dx'\,\phi(x';k_{cx})U^{(1)}_{ce}(x')\,\phi(x';k_{ex})\right)^2 \times S(k_{cy}-k_{ey}), \tag{3}$$

where $\phi(x;k_x)$ is the solution of the one-dimensional differential equation.

$$\left(\frac{d^2}{dx^2}-U^{(0)}(x)+k_x^2\right)\phi(x;k_x)=0 \tag{4}$$

which is regular or goes to zero as $x\to-\infty$ inside the slab and is normalized as

$$\phi(x;k_x)\sim\sin(k_x x+\delta)\ \ \text{as}\ \ x\to\infty. \tag{5}$$

Accepting for the moment (Appendix A) that as $k_e\to 0$ the amplitude of $\phi(x;k_{ex})$ in the internal region $x<a$ goes to zero as $k_e\sim\sqrt{\epsilon}$, then the square of the overlap integral in Eq. (3) behaves as k_e^2. Together with the $1/k_e$ prefactor we get an overall behavior of k_e for the inelastic probability as claimed.

$\phi(x;k_x)$ is the solution of a one-dimensional Schrödinger equation for the incoming particle in the one-dimensional long-range potential created by the slab. The suppression of its amplitude by $\sqrt{\epsilon}$ near the slab is due to the reflection it suffers where the interaction turns on. Within the perturbative setup the nonsticking conclusion is then already foregone.[1]

The problem is whether we can really accept this verdict of the one-dimensional unperturbed solution, when in fact we know that the turning on of the perturbation (many-body interactions) causes a multitude of resonances to be created, internal resonances being exactly the situation in which the proposition (Appendix A) above is known to badly fail. It appears that the perturbation is in no sense a small physical effect. Therefore a nonpeturbative approach is needed. Here we use R-matrix theory in its general form to accomplish the task.

IV. REDUCTION TO ONE DIMENSION AND S MATRIX

One point that the preceding section has made clear is that it is the motion and energy in the x direction which is most relevant. To better see this, imagine constraining the y motion in each open channel to be that representing specular reflection (alternatively any other fixed traveling wave mode in the y direction). The reason we may do this without affecting our final conclusions is that inclusion of the coupling to other modes simply gives additional inelastic scattering channels, which we will find are already expressed with generality in the formulation below.

The above argument is equivalent to expanding the full scattering wave function as

$$\psi(x,y,u)=\sum_{c=1}^{\infty}\left[\int_{-\infty}^{\infty}dk_y\psi_c(x,k_y)e^{ik_y y}\right]\Omega_c(u), \tag{6}$$

and including only the components

$$\overline{\psi}_c(x)\equiv\psi_c(x,k_y=k_{cy})\quad c=1,2\cdots \tag{7}$$

while solving the resulting coupled set of equations, with the potential matrix elements $U^{(\rm int)}(x,k_{cy}-k_{cy'},u)$ which couple this subset of modes.

With this understanding we may agree to simply drop all reference to the y coordinate and deal simply with the purely one-dimensional problem (in the scattering degree of freedom) that presents itself, with $V^{(\rm int)}(x,u)$ being some general interaction potential. Continuing to assume for the moment for simplicity that it is zero for $x>a$, the scattering wave function of this simplified system corresponding to the scattering particle coming in on one entrance channel, say $c=e$, with energy $\epsilon=\hbar^2k_e^2/(2m)$ is

$$\psi(x,u)=\sum_{c=1}^{\infty}\left(\frac{e^{-ik_e x}}{\sqrt{k_e}}\delta_{ce}-\frac{e^{ik_c x}}{\sqrt{k_c}}S_{ce}\right)\Omega_c(u)\quad x>a. \tag{8}$$

We exploit the following exact parametrization for the entire **S** matrix:

$$\mathbf{S}=e^{-ika}\frac{1}{1-i\sqrt{k}\mathbf{R}\sqrt{k}}(1+i\sqrt{k}\mathbf{R}\sqrt{k})e^{-ika} \tag{9}$$

(Appendix B). Here **R** the R matrix is a sum of poles

$$R_{cc'}(E)=\sum_{\lambda=1}^{\infty}\frac{\gamma_{\lambda c}\gamma_{\lambda c'}}{E_\lambda-E}, \tag{10}$$

where

$$\gamma_{\lambda c}=\sqrt{\frac{\hbar^2}{2m}}\int_{\text{all u}}du\chi_\lambda(a,u)\Omega_c(u), \tag{11}$$

and where $\chi_\lambda(x,u)$ (defined for $x\leqslant a$) are the exact bound states of the scatterer and slab system confined to $x<a$ by Neumann boundary conditions at $x=a$, with energies E_λ.

V. S MATRIX NEAR A RESONANCE

As discussed in the Introduction, the resonances are a key to the sticking issue. Sticking is essentially a long-lived Feshbach resonance in which energy has been supplied to surface and bulk degrees of freedom, temporarily dropping the scattering particle into a bound state of the attractive potential. Thus we must study resonances in various circumstances in the low incident translational energy regime. We derive the approximation for $\mathbf{S}(E)$ near $E=E_0$, a resonant energy of the compound system. E_0 is the total energy of the compound (resonant) system. Within the R-matrix approach, the compound bound states $\chi_\lambda(x,u)$ with Neumann boundary conditions at $x=a$ are properly coupled to the continuum. Some of the eigenstates are weakly coupled to the continuum, as evidenced by small values of the $\gamma_{\lambda c}$'s; these are the measure of the strength of the continuum couplings. While every one of the R-matrix bound states will result in a pole E_λ in the R matrix expansion, only the weakly coupled ones are the true long-lived Feshbach resonances of physical

interest. It is also helpful to know that the values of these ''truly'' resonant poles at E_λ are the most stable to changes in the position $x=a$ of the box. This in fact provides one unambiguous way to identify them. In Sec. V A below we first derive the resonant approximation to the **S** matrix in the vicinity of one of these Feshbach resonances when it is isolated. Then in Sec. V B we will derive the resonant approximation when the resonances are overlapping, this being by far the more physically relevant case.

A. Isolated resonance

As mentioned, the point of view we will take is to identify a resonant energy with a particular pole E_λ in the **R** matrix expansion of Eq. (B9). Those E_λ corresponding to resonances are a subsequence of the E_λ appearing in the expansion in Eq. (10). For E near a well isolated resonance at E_λ we separate the sum-over-poles expansion of the R-matrix into a single matrix term having elements $\gamma_{\lambda c}\gamma_{\lambda c'}/(E_\lambda - E)$, plus a sum over all the remaining terms, call it **N**. If the energy interval between E_λ and all the other poles is large compared to the open-open residue at E_λ then we may expect that the $n\times n$ open-open block of **N** will have all its elements be small. Then rewriting the inverse in Eq. (9)

$$\frac{1}{1-i\sqrt{k}\mathbf{R}\sqrt{k}} \equiv \frac{1}{1-i\left(\mathbf{M}+\dfrac{\mathbf{V}}{E_\lambda - E}\right)}, \tag{12}$$

where $\mathbf{M}\equiv\sqrt{k}\mathbf{N}\sqrt{k}$ and $V_{cc'}\equiv(\sqrt{k_c}\gamma_{\lambda c})(\sqrt{k_{c'}}\gamma_{\lambda c'})$, and setting $\mathbf{M}=0$ allows us to simplify the central term in Eq. (9) exactly (we will return to the case $\mathbf{M}\neq 0$),

$$\frac{1}{1-i\sqrt{k}\mathbf{R}\sqrt{k}}(1+i\sqrt{k}\mathbf{R}\sqrt{k}) \tag{13}$$

$$= 1+\frac{1}{1-\dfrac{i\mathbf{V}}{E_\lambda - E}} 2i\frac{\mathbf{V}}{E_\lambda - E} \quad (\text{with } \mathbf{M}=0) \tag{14}$$

$$= 1+\frac{1}{E_\lambda - E - i(\Gamma_\lambda/2 + i\Delta E_\lambda)} 2i\mathbf{V}k, \tag{15}$$

where we used

$$V^2 = [(\gamma_{\lambda 1}^2 k_1 + \cdots + \gamma_{\lambda n}^2 k_n) + (\gamma_{\lambda(n+1)}^2 k_{n+1} + \cdots)]\mathbf{V} \tag{16}$$

$$\equiv \left[\left(\frac{\Gamma_{\lambda 1}}{2} + \cdots + \frac{\Gamma_{\lambda n}}{2}\right) + i(\gamma_{\lambda(n+1)}^2 \kappa_{n+1} + \cdots)\right]\mathbf{V} \tag{17}$$

$$\equiv \left(\frac{\Gamma_\lambda}{2} + i\Delta E_\lambda\right)\mathbf{V} \tag{18}$$

to get the identity

$$[E_\lambda - E - iV]\mathbf{V} = [E_\lambda - E - i(\Gamma_\lambda/2 + i\Delta E_\lambda)]\mathbf{V} \tag{19}$$

$$\Rightarrow \frac{1}{E_\lambda - E - i(\Gamma_\lambda/2 + i\Delta E_\lambda)}\mathbf{V} = \frac{1}{E_\lambda - E - i\mathbf{V}}\mathbf{V} \tag{20}$$

which was used in the last step. Also define $(\Gamma_{\lambda c}/2)^{1/2} \equiv \gamma_{\lambda c}\sqrt{k_c}, c=1,2,\cdots,n$, which defines the sign of the square root on the left-hand side. Thus we arrive at

$$S_{cc'} = e^{-ik_c a}\left(\delta_{cc'} + \frac{i\Gamma_{\lambda c}^{1/2}\Gamma_{\lambda c'}^{1/2}}{E_\lambda^{(r)} - E - i\Gamma_\lambda/2}\right)e^{-ik_{c'}a}, \tag{21}$$

where $E_\lambda^{(r)} \equiv E_\lambda + \Delta E_\lambda$, for the $n\times n$ open-open unitary block of S in the neighborhood of a single isolated resonance after neglecting the contribution of the background matrix M. For us the essential point is that

$$\Gamma_{\lambda c} = 2k_c(E)\gamma_{\lambda c}^2, \tag{22}$$

i.e., the partial widths $\Gamma_{\lambda c}$ depend on the energy E, through the kinematic factor $k_c(E)$. Mostly this energy dependence is small and irrelevant except where the k_c's and hence $\Gamma_{\lambda c}$'s are varying near 0. These are the partial widths of the open channels near threshold. Hence $|S_{ce}|^2$ $(c\neq e)$, an inelastic probability, behaves like $k_e \sim \sqrt{\epsilon}$ when the entrance channel is at threshold. Including the background term $(\mathbf{M}\neq 0)$ does not change this. To see this we may perform the inverse in Eq. (9) to first order in **M** and then get an additional contribution of the terms

$$e^{-ika}\left(\frac{2i}{1-\dfrac{i\mathbf{V}}{E_\lambda - E}}\mathbf{M} + \frac{1}{1-\dfrac{i\mathbf{V}}{E_\lambda - E}} + \frac{1}{1-\dfrac{i\mathbf{V}}{E_\lambda - E}} i\mathbf{M}\frac{1}{1-\dfrac{i\mathbf{V}}{E_\lambda - E}} 2i\mathbf{V}\right)e^{-ika} \tag{23}$$

to the S matrix. Now, both **M** and **V** have a factor of $\sqrt{k_c}$ multiplying their cth columns (and rows) from their definitions and so a matrix element $b_{cc'}$ of the matrix in parentheses in Eq. (23) will have a $\sqrt{k_c}$ and $\sqrt{k_{c'}}$ dependence. An inelastic element of $S_{cc'}(c\neq c')$ would therfore take a form similar to that of Eq. (21), with the identity matrix element $\delta_{cc'}$ there being replaced by $b_{cc'}$. Since our interest is in the case when the entrance channel is at threshold this dependence is still $\sqrt{k_e}$, making the inelastic probability $|S_{ce}|^2$ still continue to behave as $k_e \sim \sqrt{\epsilon}$, even with background.

B. Overlapping resonances

Here we require the form of the **S** matrix near an energy E where many of the quasibound states may be simultaneously excited, i.e., the resonances overlap. Again, neglecting background for the moment, the **S** matrix is simply taken to be a sum over the various resonances,

$$\mathbf{S} = 1 - \sum_\lambda \frac{i\mathbf{A}_\lambda}{E - E_\lambda^{(r)} + i\Gamma_\lambda/2}, \tag{24}$$

where A_λ is a $n\times n$ rank 1 matrix with the cc'th component as $\Gamma_{\lambda c}^{1/2}\Gamma_{\lambda c'}^{1/2}$. There is no entirely direct justification of this form, but one can see that there is much which it gets correct.

The $\mathbf{A_\lambda}$ are symmetric, hence **S** is symmetric. Obviously it has the poles in the right places, allowing the existence of decaying states with a purely outgoing wave at the resonant energies. A crucial additional assumption that also makes **S** approximately unitary is that the signs of the $\Gamma_{\lambda c}^{1/2}$ are random and uncorrelated both in the index λ as well as c, regardless of how close the energy intervals involved may be. One simple consequence is that we approximately have that

$$\mathbf{A_\lambda A_{\lambda'}} = \delta_{\lambda\lambda'}\Gamma_\lambda \mathbf{A_\lambda} \tag{25}$$

in the sense that the lhs is negligible for $\lambda\neq\lambda'$ in comparison to the value for $\lambda=\lambda'$. With Eq. (25) it is easy to verify the approximate unitarity of **S**. Ultimately, the assumed randomness is traced back to the irregularity of the wave functions $\chi_\lambda(x,u)$ in the defining Eq. (11). Even if the target itself is a highly regular one must remember that these $\chi_\lambda(x,u)$ are the solutions in the full presence of the incident particle at a distance where the interaction is felt very strongly.

The random sign assumption has become quite firmly established since its inception in the early days of nuclear physics, due in part to its great success in the prediction of such quantities such as average cross sections.[15] Notably, it was used some time later in predicting the so-called Ericson fluctuations.[16] This was the slowly varying energy dependence of cross sections in the strongly overlapping regime, such as we wish to consider in this section below.

We investigate first the onset of the overlapping regime as E increases. $D(E)$, the level spacing of the resonant $E_\lambda^{(r)}$, is a rapidly decreasing function of its argument. On the other hand, $\Gamma_\lambda=\Gamma_{\lambda 1}+\Gamma_{\lambda 2}+\cdots+\Gamma_{\lambda n}$, and since more channels are open at higher energy, Γ_λ is increasing with the energy of the resonance. The widths must therefore eventually overlap, and $\Gamma_\lambda \gg D(E_\lambda^{(r)})$ for the larger members of the sequence of $E_\lambda^{(r)}$'s. In this regard there is a useful estimate due to Bohr and Wheeler,[17] that for n large,

$$\frac{\Gamma_\lambda}{D(E_\lambda^{(r)})} \simeq n, \tag{26}$$

where n is the number of open channels. Appendix C derives this using a phase space argument. Here we point out that this is entirely consistent with the assumption of the random signs, indeed it requires it to be true. Take for example a typical inelastic amplitude

$$\mathbf{S}_{cc'} = -i\sum_\lambda \frac{\Gamma_{\lambda c}^{1/2}\Gamma_{\lambda c'}^{1/2}}{E_\lambda^{(r)}-E-i\Gamma_\lambda/2} \quad (c\neq c'). \tag{27}$$

Since $\Gamma=nD$ and $\Gamma_\lambda=\Gamma_{\lambda 1}+\Gamma_{\lambda 2}+\cdots\Gamma_{\lambda n}$, it follows that the typical size of a partial width $\Gamma_{\lambda c}$ is D. Therefore the typical magnitude of $\Gamma_{\lambda c}^{1/2}\Gamma_{\lambda c'}^{1/2}$ is D, but the sign fluctuates randomly over the index λ, because of the assumed randomness of the $\Gamma_{\lambda c}^{1/2}$. Thus for energies in the overlapping domain $S_{cc'}$ is a sum of n complex numbers each of typical size $D/\Gamma=1/n$, but random in sign. This makes for a sum of order $1/\sqrt{n}$. Clearly this is the right order of magnitude required to make the $n\times n$ matrix **S** unitary.

Unlike the case of the isolated resonance, the S-matrix elements here are smoothly varying in E. Replacing the identity matrix element of Eq. (24) with a background matrix B just shifts this smooth variation by a constant. If $B_{cc'}$ is also thought of as arising from a sum over the individual backgrounds then for the same reasons as discussed at the end of the preceding section $|B_{ce}|^2\sim k_e\sim\sqrt{\epsilon}$ for an entrance channel near the threshold. For simplicity we will continue to take $B_{cc'}=\delta_{cc'}$. One may verify that the background does not affect our conclusions below.

VI. Q MATRIX AND STICKING

From the viewpoint of scattering theory, the sticking of the incident particle to the target is just a long-lived resonance. It is natural then to investigate the time delay for the collision. Smith[14] introduced the collision lifetime or Q matrix,

$$\mathbf{Q}\equiv i\hbar\mathbf{S}\frac{\partial\mathbf{S}^\dagger}{\partial E}, \tag{28}$$

which encapsulates such information. The right-hand side (rhs) of Eq. (28) involves the ''open-open'' upper left block of **S** so that **Q** is also an $n\times n$ energy-dependent matrix, having dimensions of time. If $\vec{v}$ is a vector whose entries are the coefficients of the incoming wave in each channel then $\vec{v}^{\,\mathrm{tr}}\mathbf{Q}(E)\vec{v}$ is the average delay time experienced by such an incoming wave. Because physically the particle is incident on only one channel, $\vec{v}$ consists of all 0's except for a 1 in the eth slot so that the relevant quantity is just the matrix element $\mathbf{Q}_{ee}(E)$. Smith shows that this delay time is the surplus probability of being in a neighborhood of the target (measured relative to the probability if no target were present) divided by the flux arriving in channel e. This matches our intuition that when the delay time is long, there is a higher probability that the particle will be found near the target.

Now as a Hermitian matrix, $\mathbf{Q}(E)$, can be resolved into its eigenstates $\vec{v}^{(1)}\cdots\vec{v}^{(n)}$ with eigenvalues $q_1\cdots q_n$. The components of $\vec{v}^{(1)}$ are the incoming coefficients of a quasi-bound state with lifetime q_1 and so on. Then

$$\vec{v}^{\,\mathrm{tr}}\mathbf{Q}(E)\vec{v} = \sum_{j=1}^{n} q_j|\vec{v}^{(j)}\cdot\vec{v}|^2. \tag{29}$$

As can be seen from this expression, the average time delay results, in general, from the excitation of multiple quasistuck states each with its lifetime q_j and probability of formation $|\vec{v}^{(j)}\cdot\vec{v}|^2$. However, we will find that using our resonant approximation to the **S** matrix near a resonant energy $E_\lambda^{(r)}$ the time delay will consist of only one term from the sum on the rhs of Eq. (29), all the other eigenvalues being identically 0.

Using Eq. (28),

$$\mathbf{Q}(E)=i\hbar\left(\sum_{\lambda'}\frac{-iA_{\lambda'}}{[E-E_{\lambda'}^{(r)}-i\Gamma_{\lambda'}/2]^2}-\sum_{\lambda\lambda'}\frac{A_\lambda A_{\lambda'}}{[E-E_\lambda^{(r)}+i\Gamma_\lambda/2][E-E_{\lambda'}^{(r)}-i\Gamma_{\lambda'}/2]^2}\right) \tag{30}$$

which using Eq. (25) simplifies to

$$=\sum_\lambda\frac{\hbar}{(E-E_\lambda^{(r)})^2+(\Gamma_\lambda/2)^2}A_\lambda, \tag{31}$$

a remarkably simple answer. We need $Q_{ee}(E)$, where e is the entrance channel,

$$Q_{ee}(E)=\sum_\lambda\frac{\hbar\Gamma_{\lambda e}}{(E-E_\lambda^{(r)})^2+(\Gamma_\lambda/2)^2} \tag{32}$$

$$=\sum_\lambda\left(\frac{\hbar\Gamma_\lambda}{(E-E_\lambda^{(r)})^2+(\Gamma_\lambda/2)^2}\times\frac{\Gamma_{\lambda e}}{\Gamma_\lambda}\right), \tag{33}$$

where the second equation has the interpretation (for each term) as the lifetime of the mode, multiplied by the probability of its formation. Note how for each resonance $E_\lambda^{(r)}$ there is only one term corresponding to the decomposition of Eq. (29). The actual measured lifetime is the average of $Q_{ee}(E)$ averaged over the energy spectrum $|g(E)|^2$ of the collision process.

A. Energy averaging over spectrum

With the target in state $\Omega_e(u)$ where $c=e$ is the entrance channel, the energy of the target is fixed, and the time-dependent solution will look like

$$\psi(x,u,t)=\int dE\left[g(E)\sum_{c=1}^{\infty}\left(\frac{e^{-ik_c(E)x}}{\sqrt{k_e(E)}}\delta_{ce}-\frac{e^{ik_c(E)x}}{\sqrt{k_c(E)}}S(E)_{ce}\right)\Omega_c(u)\right]. \tag{34}$$

Recall, E is the total energy of the system. We are interested in the threshold situation where the incident kinetic energy of the incoming particle $\epsilon\to 0$. This can be arranged if $g(E)$ is peaked at E_0 with a spread ΔE such that (i) E_0 is barely above E_e^{target} and (ii) $\Delta E=\delta\epsilon$ is some small fraction of ϵ, the mean energy of the incoming particle. The second condition ensures that we may speak unambiguously of the incoming particle's mean energy. So,

$$\langle Q_{ee}(E)\rangle\equiv\int dE|g(E)|^2Q_{ee}(E) \tag{35}$$

$$\simeq\frac{1}{\Delta E}\int dEQ_{ee}(E); \tag{36}$$

$\langle\rangle$ denotes the average over the ΔE interval. Now $Q_{ee}(E)$ is just a sum of Lorentzians centered at the $E_\lambda^{(r)}$'s with width Γ_λ and Eq. (36) is just a measure of their mean value over the ΔE interval.

So long as the ΔE interval around which we are averaging is broad enough to straddle many of these Lorentzians, the mean height is just

$$\frac{1}{\Delta E}\times\rho(E)\Delta E\times\frac{\hbar\pi\Gamma_{\lambda e}}{\Gamma_\lambda}, \tag{37}$$

where the third factor is the area under the "λth" Lorentzian. This is true regardless of whether or not they are overlapping. It will be convenient to write Γ_λ as

$$\Gamma_\lambda=n\times 2\overline{k_\lambda}\,\mathrm{var}(\gamma_\lambda), \tag{38}$$

where $\mathrm{var}(\gamma_\lambda)$ is the variance of the set of $\gamma_{\lambda c}$'s over the n open channels and $\overline{k_\lambda}$ is a mean or effective wave number k_c over the open channels, which for a particular realization λ we take to be defined by Eq. (38) itself. Let $\langle\rangle$ denote the average over the occurrences of the quantity in the ΔE interval. $\Gamma\equiv\langle\Gamma_\lambda\rangle$, $\overline{k}\equiv\langle\overline{k_\lambda}\rangle$. Then Eq. (37) simplifies to

$$\langle Q_{ee}(E)\rangle\simeq\hbar\frac{1}{D}\frac{k_e\langle\gamma_{\lambda e}^2\rangle}{n\overline{k}\langle\mathrm{var}(\gamma_\lambda)\rangle} \tag{39}$$

$$\simeq\frac{\hbar}{\Gamma}\frac{k_e}{\overline{k}} \tag{40}$$

which tends to 0 as $k_e\sim\sqrt{\epsilon}$. The form of Eq. (40) and all the steps leading up to it remain valid whether the Lorentzians are overlapping or not, as long as the $\Delta E=\Delta\epsilon$ interval which we are averaging over includes many of them.

B. On an isolated resonance

If the target is cold enough that the resonances are isolated, then as the incident particle's energy $\epsilon\to 0$, adhering to the condition $\Delta\epsilon<\epsilon$ will eventually result in $\Delta\epsilon$ becoming narrower than the resonance widths. It becomes possible then for $\Delta\epsilon$ to be centered right around a single isolated resonance at $E_\lambda^{(r)}$. In this case $\langle Q_{ee}(E)\rangle$ is found simply by putting $E=E_\lambda^{(r)}$, because the spectrum $|g(E)|^2$ is well approximated by $\delta(E-E_\lambda^{(r)})$. So

$$\langle Q_{ee}(E)\rangle=\frac{\hbar\Gamma_{\lambda e}}{\Gamma_\lambda^2}=\frac{\hbar}{\Gamma_\lambda}\frac{\Gamma_{\lambda e}}{\Gamma_\lambda}=\frac{\hbar}{\Gamma_\lambda}\frac{k_e}{n\overline{k}}. \tag{41}$$

Even in this case there is the $\sqrt{\epsilon}$ behavior as $\epsilon\to 0$ and there is no sticking.

In the extreme case that there are no other open channels at all $(n=1)$, $\langle Q_{ee}(E)\rangle\simeq\hbar\Gamma_{\lambda e}/\Gamma_\lambda^2=\hbar/\Gamma_{\lambda e}$ because $\Gamma_\lambda=\Gamma_{\lambda e}$. In fact, $e=1$, and $\langle Q_{ee}(E)\rangle$ diverges, implying in this case that it is possible to have the particle stick. This is an exception to all the cases above but is experimentally not so relevant because we may always expect to find some exothermic channels open for a target with many degrees of freedom.

VII. INELASTIC CROSS SECTIONS AND STICKING

Another physically motivated measure of the sticking probability may be obtained by studying the total inelastic cross section of the collision. The idea is that any long-lived ''sticking'' is overwhelmingly likely to result in an inelastic collision process; i.e., that the scattering particle will leave in a different channel than it entered with. Using the original Wigner approach it is possible to show that for our case where we have only one scattering degree of freedom, the inelastic probability for an exothermic and endothermic collision vanishes like k_e. The only possible exception to this is a measure zero chance of a resonance exactly at the threshold energy E_e^{target}. In the event that there is a resonance $E_\lambda^{(r)}$ close to but above this threshold energy, it is only necessary that E is below $E_\lambda^{(r)}$ (by an energy of at least ΔE, the spread in energy) in order to observe the usual Wigner threshold behavior:

$$P_{\text{inelastic}} \to 0 \quad \text{like} \quad k_e \propto \sqrt{\epsilon}, \tag{42}$$

for the inelastic probability. However, our problem is unusual in the sense that because of the large number of degrees of freedom of the target, we will always find resonances between E_e^{target} and E no matter how small $E - E_e^{\text{target}} = \epsilon$ is. Thus the Wigner regime is not accessible. Still the surprise is that a simple computation reveals that the same behavior holds for large n:

$$P_{\text{inelastic}}(E) = \sum_{c \neq e} P_{c \leftarrow e}(E) \tag{43}$$

$$= \sum_{c \neq e} |S_{ce}(E)|^2 \tag{44}$$

$$= \sum_{c \neq e} \sum_{\lambda} \sum_{\lambda'} \frac{{\Gamma_{\lambda c}}^{1/2} {\Gamma_{\lambda e}}^{1/2}}{E - E_\lambda^{(r)} - i\Gamma_\lambda/2} \frac{{\Gamma_{\lambda' c}}^{1/2} {\Gamma_{\lambda' e}}^{1/2}}{E - E_\lambda^{(r)} + i\Gamma_\lambda/2} \tag{45}$$

$$\Rightarrow P_{\text{inelastic}}(E) = \sum_{\lambda} \frac{\Gamma_\lambda}{(E - E_\lambda^{(r)})^2 + (\Gamma_\lambda/2)^2} \Gamma_{\lambda e}, \tag{46}$$

where we used the random sign property of the $\Gamma_{\lambda c}^{1/2}$'s and the understanding that $\Sigma_{c \neq e} \Gamma_{\lambda c} \simeq \Sigma_{\text{all } c} \Gamma_{\lambda c} = \Gamma_\lambda$. Since the sum $\Sigma_{c \neq e}$ is over the $n \gg 1$ open channels, omission of a single term can hardly matter. Apart from the factor $\hbar/\Gamma_\lambda$, the rhs of the above equation is identical to the expression for $Q_{ee}(E)$ in Eq. (33). Averaging $P_{\text{inelastic}}(E)$ over many resonances $E_\lambda^{(r)}$ (overlapping or not) we may use the same algebraic simplifications as before to show

$$\langle P_{\text{inelastic}} \rangle = \frac{k_e}{\overline{k}}. \tag{47}$$

As k_e tends to 0, this gives the $\sqrt{\epsilon}$ Wigner behavior showing that there is no sticking.

The above argument fails when there is only one open channel. There are no inelastic channels to speak of. In this case, if the energy E coincides with a resonant energy $E_\lambda^{(r)}$ we will have the exceptional case of sticking, as discussed at the end of the previous section. But as pointed out there, this is primarily of theoretical interest only.

VIII. CHANNEL DECOHERENCE

The only case for which the particle sticks is seen to be the case when we are sitting right on top of a resonance with the incoming energy so well resolved that we are completely within the resonance width, *and* there are no exothermic channels open. Having no such channels open amounts to an infintesimally low energy for a large target. Otherwise, the sticking probability tends to 0 as $\sqrt{\epsilon}$ in every case.

A. Time-dependent picture

From the time-independent point of view, the physical reason for the absence of low-energy sticking is contained in the factor $\Gamma_{\lambda e}/\Gamma_\lambda$ of Eq. (33). This is the formation probability for the compound state. We will explain physically why it is small for $n \gg 1$. The resonance state is a many-body entangled state. If we imagine the decay of this compound state (already prepared by some other means, say) each open channel carries away some fraction of the outgoing flux, with no preference for any one particular channel. Running this whole process in reverse it becomes evident that the optimum way to *form* the compound state is to have each channel carry an incoming flux with exactly the right amplitude and phase. This, however, corresponds to an entangled initial state. With all the incoming flux instead constrained to be in only one channel it becomes clear that we are not exciting the resonance in the optimal way and the buildup of amplitude inside is not so large; i.e., the compound state has a small probability of forming.

The time-dependent view is even more revealing. Imagine a wave-packet incident on the system. For a single open-channel Feshbach resonance, the buildup of amplitude in the interior region can be decomposed as follows. As the leading edge of the wave packet approaches the region of attraction, most is turned away due to the quantum reflection phenomena. (It is a useful model to think of the quantum reflection as due to a barrier located some distance away from the interaction region.) The wave function in the interaction region constructively interferes with new amplitude entering the region. At the same time, the amplitude leaving the region is out of phase with the reflected wave, canceling it and assisting more amplitude to enter. The result is a large buildup of probability in spite of the effective barrier; i.e., a resonance.

Now suppose many channels are open. All the flux entering the interior must of course return, but it does so fragmented into all the other open channels. Only the fraction that makes it back into the entrance channel has the opportunity to interfere (constructively) with the rest of the entering wave packet. The constructive interference is no longer efficient and is in fact almost negligible for $n \gg 1$, thereby ruining the delicate process that was responsible for the buildup of the wave function inside. The orthogonality of the

other channels prevents interference in the scattering dimension. If we trace over the target coordinates, leaving only the scattering coordinate, most of the coherence and the constructive interference is lost, and no resonant buildup occurs. Therefore one way to understand the nonsticking is to say that decoherence is to blame.

B. Fabry-Perot and measurement analogy

Suppose we have a resonant quantum-mechanical Fabry-Perot cavity, where the particle has a high probability of being found in between the two reflecting barriers. Now, during the time it takes for the probability to build up in the interior, suppose we continually measure the position of the particle inside. In doing so we decohere the wave function and in fact never find it there at all. Alternatively, imagine simply tilting one barrier (mirror) to make it nonparallel to the first and redirecting the flux into an orthogonal direction, again spoiling the resonance. Measurement entangles other (orthogonal) degrees of freedom with the one of interest, resulting in flux being effectively redirected into orthogonal states. Thus the states of the target (if potentially excitable) are in effect continually monitoring (measuring) to see if the incoming particle has made it in inside, ironically then preventing it from ever doing so. The buildup process of constructive interference in the interaction region, described in the preceding paragraph, is slower than linear in t. Therefore the constant measurement of the particle's presence (and resultant prevention of sticking) is an example of the Zeno ''paradox'' in measurement theory.

All this does not tell us much about how sticking turns on as the incident translational energy is raised. Moreover, predicting the sticking probabilities quantitatively requires knowledge of the long-range form of the potential. This is the subject of the following sections of our paper, where a WKB analysis proves very useful. Quantum reflection is a physical phenomenon linked directly to the failure of the WKB approximation.

IX. QUANTUM REFLECTION AND WKB

Let us consider the typical case of an attractive potential arising out of the cumulative effect of van der Waals attractions between target and incident atoms. A classical atom would proceed straight into the interaction region showing no sign of reflection, but the quantum-mechanical probability of being found inside is suppressed by a factor of k (as $k \to 0$) as compared to the classical probability (see Secs. III and XIII), where k is the wave vector of the incoming atom. (Since we are dealing with one body wave functions, from here on we will suppress the subscript ''e'' on the wave number k.) This is tantamount to saying that quantum mechanically the amplitude is reflected back without penetrating the interaction region, analogous to the elementary case of reflection from the edge of a step-down potential in one dimension while attempting to go over the edge. A useful way to view this is to attribute the reflection to the failure of the WKB approximation.

To be specific, we keep the geometry of Sec. II in mind.

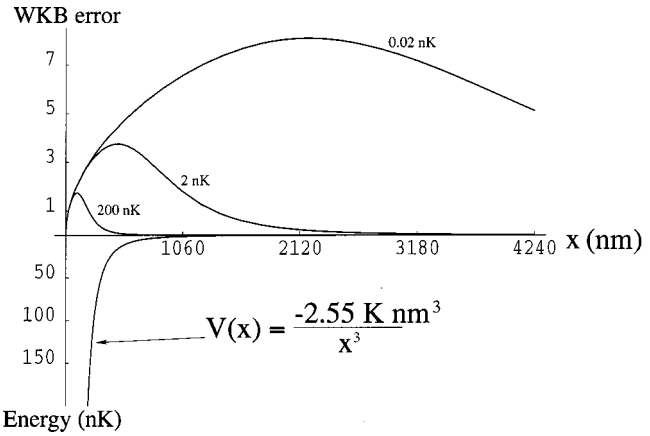

FIG. 3. The WKB error of Eq. (48) for three different values of the incoming energy 200, 2, and 0.02 nK, vs the distance x nm from the slab (SiN). The long-range form of the potential $-c_3/x^3$ ($c_3 = 220$ meV Å^3) is also shown for which the negative ''y axis'' is calibrated in the different units of energy. The sticking probabilities for the three cases are approximately 1, 0.6, 0.1.

For a low incoming energy $\epsilon \equiv \hbar^2 k^2/2m$, a left-moving WKB solution begun well inside the interaction region will fail to match onto a purely left-going WKB solution as we integrate out to large distances because the WKB criterion

$$|\lambda'(x)| = \left| \frac{\hbar p'}{p^2} \right| \ll 1 \tag{48}$$

for the local accuracy of the wave function will in general fail to be valid in some intermediate region. For bounded potentials that turn on abruptly, for example at $x=a$, it is obvious that WKB will fail near $x \sim a$. For long-range potentials such as a power law $V(x) = -c_n/x^n$ it is not immediately obvious where this region of WKB failure lies, if it exists at all. It turns out that even in this case it is possible to identify (for small enough ϵ) a distance (dependent on ϵ) at which the potential ''turns on'' and where WKB will fail. We will show below that WKB is at its worst [$|\lambda'(x)|$ is maximized] at a distance x where the kinetic and potential energies are approximately equal, i.e., where $|V(x)| \sim \epsilon$. The distance away from the slab at which the particle is turned around—or quantum reflected—is precisely this distance. Furthermore, one may heuristically expect that the greater the failure of WKB, the greater the reflection.

Figure 3 shows a plot of the error term in Eq. (48) for three different values of the incoming energy of neon on a semi-infinite slab of SiN. The essential points to notice are:

(i) There is a greater error incurred in attempting to apply the WKB (classical mechanics) approximation to colder atoms than to warmer ones. Consequently, we expect that the slower the atom, the more nonclassical its behavior. In particular, slow enough atoms will be ''quantum reflected'' and will not stick.

(ii) As the incoming velocity is decreased the atom is reflected at distances progressively further and further away

from the slab. This is because the interval in x around which the WKB error is large, may be identified as the region from which the atom is reflected.

A useful qualitative rule of thumb obtained in Sec. X below is that the region of WKB error reaches all the way out to those regions where the potential energy is still roughly the same order of magnitude as the incoming energy [Eq. (52)]. This means that as $\epsilon \to 0$ the error is still large where the potential energy graph looks essentially flat. In fact as $\epsilon \to 0$ it is easily shown that a plot of the WKB error will show a nonuniform convergence to a polynomial proportional to

$$x^{n/2-1} \quad \text{for all} \quad n>0 \tag{49}$$

Figure 3 shows the case for $n=3$.

X. WKB FAILURE

Differentiating $p^2/2m+V(x)=\epsilon$ with respect to x, we have

$$p' = \frac{-mV'}{p} \tag{50}$$

which when used repeatedly to eliminate p' shows that $|p'/p^2|$ in Eq. (48) is maximized when

$$\frac{p^2}{3m} = \frac{V'^2}{V''}. \tag{51}$$

For $V(x)=-c_n/x^n$, this is exactly when

$$|V(x)| = \epsilon\left(\frac{2(n+1)}{n-2}\right). \tag{52}$$

We discover that for $n>2$ only, we have a point where WKB is at its worst at a distance x where $|V(x)| \sim \epsilon$, and moreover, that this maximum behaves like

$$\max\left|\frac{p'}{p^2}\right| \sim \frac{1}{c_n^{1/n}\epsilon^{1/2-1/n}} \sim \frac{1}{c_n^{1/n}k^{1-2/n}} \tag{53}$$

which for $n>2$ diverges as $k \to 0$. Note how a *weaker* potential (smaller c_n) is *better* at reflecting a particle at the same energy, but allows the atom to approach closer. Heuristically a sketch of $V(x)=-c_n/x^n$ reveals why: the weaker potential is seen to turn on more abruptly at a point closer to $x=0$, promoting an greater breakdown of WKB there. Alternatively a simple scaling argument with Schrodinger's equation reveals the same trend.

The above conclusions are valid only for $n>2$. For $n \leqslant 2$ the error term of Eq. (48) looks qualitatively different from that in Fig. 3. It is small at all distances except near $x=0$ where it diverges to infinity, as is evident from Eq. (49). If the physical parameters are such that this region where WKB fails very close to the slab is never actually manifest in the long-range part of the potential then the "no-reflection" classical behavior will be valid all the way up to distances near the slab where the atom will begin to feel the short-range forces and lose energy to the internal degrees of freedom. For such a case then with $n<2$ we believe one will *not* observe quantum reflection.

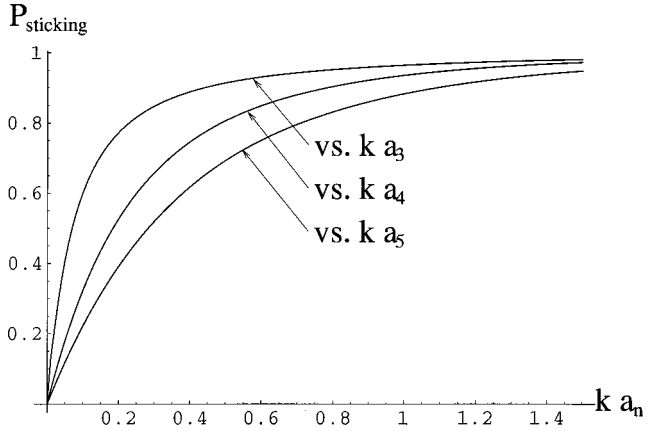

FIG. 4. Sticking probabilities for an atom incident on surface providing a long-range interaction of the form $V(x)=-c_n/x^n$ for the cases $n=3$, 4, 5. Note that the length scale a_n used to compute the dimensionless ka_n coordinate on the "x axis" vs which we plot the sticking probabilities is different for each n.

XI. STICKING PROBABILITY

Having established that the reflection is caused by a well-defined localized region, we solve the one-dimensional Schrodinger equation around this region to accurately compute the reflection probability. For an attractive power-law potential $V(x)=-c_n/x^n$, the relevant one-dimensional equation is

$$\left(\frac{d^2}{dx^2} + \frac{a_n^{n-2}}{x^n} + k^2\right)\phi_e(x) = 0. \tag{54}$$

$\phi_e(x)$ is the entrance channel wave function. The length scale

$$a_n \equiv (2mc_n/\hbar^2)^{1/(n-2)}, \tag{55}$$

contains all the qualitative information about the reflection. Its relevance is twofold. First, the sticking probability for small k, behaves as

$$P_{\text{sticking}} \sim N_n k a_n, \tag{56}$$

where N_n is a pure numeric constant (roughly of order 10 for $n=3$, and of order 1 for $n=4,5$), see Ref. 20. P_{sticking} may be computed numerically for any k, and Fig. 4 shows P_{sticking} vs ka_n for $n=3,4$, and 5. Second, the distance at which the particle is turned around is estimated by solving

$$\left(\frac{a_n}{x}\right)^n = (ka_n)^2 \tag{57}$$

for x, which is just the requirement that $|V(x)|=\epsilon$. Equation (56) together with Eq. (55) makes plain that a smaller c_n is more conducive to making quantum reflection happen, while

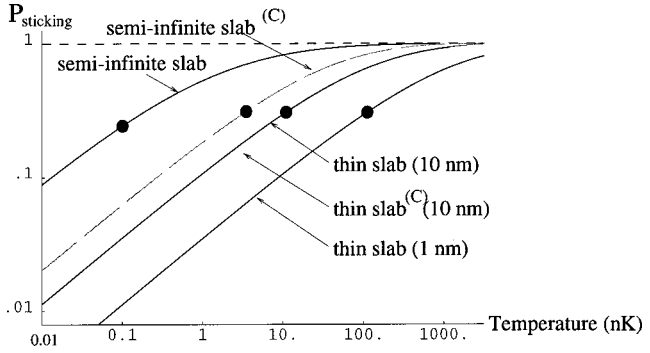

FIG. 5. Sticking probabilities vs temperature of incident Ne atoms on SiN. The broken line indicates the inclusion of the very long-range Casimir forces (see text). The large dot demarcates the regions of threshold and postthreshold, using the criterion suggested at the end of Sec. XII.

Eq. (57) indicates that the turnaround point is then necessarily closer to the surface. With these effects in mind, we look at some specific cases.

XII. EXAMPLES

We examine the case of incidence on a slab which may be treated as semi-infinite, and also the case when it is a thin film. It is useful to first look at these cases pretending there is no Casimir interaction, and assuming that the short-range form of the potential is everywhere valid. Afterwards we put in the Casimir interaction. For clarity we will pick a specific example of target and incident atoms for most of our discussions, by specifying the numeric values for the short-range potential between the atom and semi-infinite slab, since these are most comprehensively tabulated in Ref. 18.

Figure 5 shows the sticking probability vs the temperature of an incoming Ne atom in units of 10^{-9} K. The slab is silicon-nitride (SiN). The various curves are for the different cases depending on whether we are considering a thick or thin slab, and whether the Casimir effect is included or not. We will discuss these cases below, pointing out the relevant length and energy scales involved in deciding to label the slab as semi-infinite or thin. The mapping from the mathematically natural ka_n (with $n=3$ and $c_3=220$ meV Å^3) scale of Fig. 4 to the more physical temperature scale of Fig. 5 is made using

$$T \simeq [69.08\ \text{K}] \left(\frac{m_H}{m_{\text{atom}}}\right)^3 \left(\frac{\text{meV Å}^3}{c_3}\right)^2 (ka_3)^2, \quad (58)$$

where we used $\langle \epsilon \rangle = (3/2)k_B T$ to compute the temperature by setting $\langle \epsilon \rangle$ equal to the incoming energy. $m_H =$ mass of hydrogen atom and for our example $m_{\text{Ne}} = 20.03\ m_H$.

All the graphs in Fig. 5 have an initial slope of 0.5 indicating the $\sqrt{\epsilon}$ behavior of the sticking probabilities once the energies are low enough to be in the quantum reflection regime. A particular temperature at which there is a transition to the post-threshold sticking regime, we arbitrarily (but intuitively) define as the temperature where the slope becomes 0.4. For the thin-film case of 10 nm in our example this temperature is 10 nK.

While the parameters in our example are fairly typical, it is clear that the cubic dependence on mass and quadratic dependence on the c_3 coefficient in Eq. (58) will make this temperature range over quite a few orders of magnitude. The c_3's in Ref. 18, listed in units of meV Å^3 for a variety of surface atom pairs, range in values from 100 to 3000.

A. Semi-infinite slab (without Casimir)

Even though c_3 coefficients are known both theoretically and experimentally for many surface-atom pairs, for completeness we take a moment to look at a quick way of estimating them. This is provided by the London formula

$$V_{\text{atom-atom}}(r) = \frac{-3}{2} \frac{I_A I_B}{I_A + I_B} \frac{\alpha_A \alpha_B}{r^6} \equiv \frac{-c_6}{r^6}, \quad (59)$$

which estimates the van der Waals interaction between any two atoms. I is the ionization potential and α the polarizability of each atom. Then summing over all the atoms in the semi-infinite slab (thick) we get

$$V_{\text{slab-atom}}(x) = \frac{-\pi c_6 \rho_{\text{atoms}}}{6} \times \frac{1}{x^3} \equiv \frac{-c_3}{x^3}, \quad (60)$$

where $\rho_{\text{atoms}} =$ the density of slab atoms. These estimates are not very accurate, but correctly indicate the physical quantities on which the answer depends. As mentioned, Ref. 18 provides a useful compendium of these coefficients. We have used $c_3 = 220 \pm 4$ meV Å^3 for neon atoms incident on silicon nitride from work of Ref. 19. This choice of c_3 makes

$$a_3 \simeq 212 \text{ nm}. \quad (61)$$

Thus the ''semi-infinite slab'' curve of Fig. 5 is the $n=3$ curve of Fig. 4 scaled to temperature units using Eq. (58).

B. Thin slab (without Casimir)

From far enough away any slab will appear thin. The surface-atom interaction will behave like

$$\frac{-c_3}{x^3} - \frac{-c_3}{(x+d)^3} \simeq \frac{-3dc_3}{x^4} \quad (62)$$

for $x \gg d$, where d is the thickness of the slab. The resulting c_4 coefficient equal to $3dc_3$ gives an a_4 coefficient that can be written as

$$a_4 = \sqrt{\frac{2m}{\hbar^2} 3dc_3} = a_3 \left[\frac{3d}{a_3}\right]^{(1/2)}. \quad (63)$$

For macroscopic values of $d(\gg a_3)$ then, it is only for vanishingly small incident energies that the finiteness of the slab becomes apparent. For any macroscopic d this will be physically irrelevant. For microscopic $d(\ll a_3)$, however, this window in energy over which the thinness of the slab makes an appreciable difference can be larger and even prevail for all energies. To continue our illustrative example we pick the microscopic value of $d=10$ nm. This makes $a_4 \simeq 800$ nm. The ''thin slab'' curve of Fig. 5 shows that the

sticking probabilities are substantially reduced and the onset of quantum reflection occurs at a much higher energy.

As a benchmark case, we also include what will likely be the physically limiting case for a continuous film of $d=1$ nm. This further reduces the sticking probabilities for a fixed temperature by a factor of $\sqrt{10}$, because the important quantity a_4 is reduced by this much [Eq. (63)]. The transition temperature appears to have increased by three orders of magnitude versus the semi-infinite case.

C. Semi-infinite slab (Casimir regime)

As the incoming energy ϵ tends to 0, we have seen that the turnaround region from which the atom ''quantum reflects'' moves progressively further away from the slab. At large distances, however, it is well known that the interaction potential itself takes on a different form due to Casimir effects. In particular, a semi-infinite dielectric slab (dielectric constant ϵ_s) has an interaction potential with an atom of polarizability α given by

$$V_{\text{slab-}atom}(x)=\frac{-3}{8\pi}\frac{\hbar c\alpha}{x^4}\frac{\epsilon_s-1}{\epsilon_s+37/23} \quad x\to\infty \tag{64}$$

$$=\frac{-235(\text{eV}-\text{Å})\alpha}{x^4}\frac{\epsilon_s-1}{\epsilon_s+37/23} \quad x\to\infty \tag{65}$$

Even for sufficiently large x, the form above is not exact but a good approximation found in Ref. 21. Our purpose here is only to estimate the various numbers to see their relevance. It will suffice to put $\alpha_{Ne}=0.39\text{Å}^3$ and the last factor involving ϵ_s is replaced by 1 since most solids and liquids have ϵ_s substantially greater than 1. This gives a $c_4^{(C)}$ coefficient of 9×10^4 meV Å^4 and hence a resulting $a_4^{(C)}=93$ nm. The superscript ''C'' reminds us it is due to the Casimir interaction which is valid only for large enough x.

To estimate the distance beyond which the Casimir form itself is valid, we use the statement from Ref. 22: ''Within a factor of 2, the van der Waals potential is correct at distances less than $0.12\lambda_{tr}$, while the Casimir potential is correct at distances at longer range.'' $\lambda_{tr}=(1240\ \text{nm})/(\Delta E/\text{eV})$ here is the wavelength associated with the transition between the ground and excited state that gives the atom its polarizability. ΔE is the transition energy measured in eV. Knowing this much we may deduce the qualitative features of the sticking probability curve the arguments being similar to the cases above.

For this Casimir case and the one below, however, there is a caveat. The exact manner in which the potential changes its near range form to its long-range Casimir form can certainly affect the sticking probabilities at the intermediate energy where it makes this transition. Some numerical experimentation choosing arbitrary forms of the potential having the correct short-range and long-range behavior confirms this. Therefore the curves in Fig. 5 involving Casimir forces are only quantitatively and *not* qualitatively correct.

D. Thin slab (Casimir regime)

Even for a thin slab we expect that the distance at which the Casimir interaction is valid remains the same as for a semi-infinite slab made of the same material. At these distances if $x\gg d$ is also valid, then one may expect the surface atom interaction to behave like

$$\frac{-c_4^{(C)}}{x^4}-\frac{-c_4^{(C)}}{(x+d)^4}\simeq\frac{-4dc_4^{(C)}}{x^5}. \tag{66}$$

The length scale

$$a_5^{(C)}=a_4^{(C)}\left[\frac{4d}{a_4^{(C)}}\right]^{1/3} \tag{67}$$

associated with this $c_5=4dc_4^{(C)}$ coefficient makes $a_5^{(C)}=717$ nm. Figure 5 shows a slight decrease in the sticking probabilities, the effect being evidently less here than in the case of the thick slab.

E. Hydrogen on "thick" helium

Rather atypical, but extremely favorable parameters ($c_3=18$ meV Å^3) are found in the case of hydrogen atoms incident on bulk liquid helium. Evidence for quantum reflection was experimentally seen in this system.[23] The following is a comparison with the parameters used in our example of Ne on SiN:

$$m_{\text{Ne}}/m_H=20.03 \ \text{ and } \ c_3^{(\text{Ne-}SiN)}/c_3^{(\text{H-}He)}=220/18. \tag{68}$$

Using these along with Eq. (58), we see that the sticking probabilities for this case are in fact the same curves as in Fig. 5 except shifted to the right in temperature by about 6.1 orders of magnitude. This puts it exactly in the milli-Kelvin regime where sticking probabilities of about 0.01–0.03 were observed as temperatures ranged from about 0.3 to 5 mK.[23] However, the sticking probabilities predicted by the ''semi-infinite slab$^{(C)}$'' curve of Fig. 5 are about a factor of 2.5 too large, but we feel there is good reason for this. We already mentioned the qualitative manner in which the Casimir forces were included but it seems that a greater error is caused for another reason. The length scale $a_3=17$ nm for H-He is so small that the WKB error is close in (see Fig. 3) where the interaction potential is not exactly of the form $\sim1/x^3$. Practically speaking this means that the region over which we must integrate Eq. (54) must include points close to the slab to get some convergence and thus we are violating the assumption that the potential is $\sim1/x^3$ there. This problem would not plague the Ne-SiN case too much, because the length scale there is substantially bigger. For H-He we must include some short-range information to get an improvement. Still it is the long-range forces that are mostly responsible. Reference 24 and others have modeled this close range behavior and obtained better agreement; the improvement coming from explicit consideration of the bound states supported by the close range potential. These appear in the potential matrix elements of perturbation theory.

XIII. RELATION TO THRESHOLD BEHAVIOR

We now wish to take a broader view of the quantum reflection behavior at threshold ($k\to 0$), and the sticking that sets in as the energy is increased—a postthreshold behavior. In particular we want to make connection to, and extend the well-known threshold behaviors of inelastic rates which were first stated most generally by Wigner in Ref. 25. For example, Wigner showed that the exothermic excitation rates for collisions between two bodies with bound internal degrees of freedom tend to a constant value as their relative translational energy tends to 0, provided there is no resonance at the 0 translational energy threshold. Equivalently, the exothermic inelastic cross section diverges as $1/v$, a fact known in the still older literature as the "$1/v$ law." v is the relative velocity of the collision. Notice especially the proviso in the statement above, that there be no resonance at the threshold energy; suggesting that the many resonances between 0 and ϵ provided by a many-body target could make the law inoperative. But the first part of this paper established quite generally that in this many-resonance regime the $1/v$ law is reinstated.

Here we re-examine the Wigner behavior from a different point of view using our understanding of quantum reflection. In addition to furthering an intuitive understanding of the Wigner behavior, viewing things in this way will lead naturally to predicting a generic postthreshold behavior (e.g., the $1/v$ law is replaced by a $1/v^2$ law) and an understanding of when the sticking sets back in as ϵ is increased.

We shift our attention to a three-dimensional geometry of incidence on a localized cluster instead of the one-dimensional case of incidence on a slab. So long as the target dimensions are dwarfed by the incidence wavelength we will find that both problems are effectively one dimensional because it is only the *s* wave which can penetrate the interaction region. For clarity we will deal with both cases separately.

Threshold and postthreshold inelastic cross sections

The starting point is the template provided by the Golden Rule,

$$d\sigma_{e\to c}\propto\frac{1}{k}\rho(E_c)\left|\int_{\text{all r}}d^3r\,\phi^{(-)}_{c,\vec{k}_c}(\vec{r})U_{ce}(\vec{r})\,\phi^{(+)}_{e,\vec{k}}(\vec{r})\right|^2 \tag{69}$$

for the differential cross section for inelastic transitions from internal state $\Omega_e(u)$ to $\Omega_c(u)$ where $\vec{k}$ and $\vec{k}_c$ are the incoming and outgoing directions of the incident atom. We describe briefly how Eq. (69) is arrived at.

For each internal state $\Omega_c(u)$ ($c=1,2,\ldots n$) that we may imagine freezing the target in (u incorporates all the target degrees of freedom), there is some effective potential felt by the incoming atom. These potentials are just the diagonal elements of the complete interaction potential $U(x,u)$ in the $\Omega_c(u)$ basis, which if present all by themselves (off-diagonal elements 0) could only cause an elastic-collision to occur. It is the off-diagonal elements that may be thought of as causing the inelastic transitions. Treating them as a perturbation on the elastic-scattering wave functions we use the Golden Rule to obtain Eq. (69). $\rho(E)$ is the energy density of states of the free atom. $\phi^{(+)}_{e,\vec{k}}(\vec{r})$ is the entrance channel wave function and $\phi^{(-)}_{c,\vec{k}_c}(\vec{r})$ is the final channel wave function. They are both exact elastic-scattering wave functions in the potentials $U_{ee}(\vec{r})$ and $U_{cc}(\vec{r})$, respectively. The factor of $1/k$ divides the Golden Rule rate by the flux to get the probability.

Now all the k dependence of $d\sigma_{e\to c}$ and hence $\sigma_{e\to c}$ is due to (i) the factor $1/k$, and (ii) the sensitive k dependence of the amplitude of the entrance channel wave function inside the interaction region over which the overlap integral of Eq. (69) takes place. This is simply because the incoming amplitude is more reflected away by the potential as $k\to 0$ resulting in the interior amplitude being suppressed by a factor of k as compared to what one would expect classically.

1. Incidence on a slab

For this one-dimensional situation we speak of an inelastic probability instead of a cross section, but otherwise Eq. (69) remains entirely valid here also with the obvious modifications.

For $k\to 0$, when WKB is invalid, we established quite generally that the entrance channel wave function $\phi_e(x)$ when normalized to have a fixed incoming flux, had its amplitude inside the interaction region behaving like

$$\phi_e(x_{\text{inside}})\sim k \quad \text{threshold.} \tag{70}$$

Now the change from quantum reflection at threshold to sticking at postthreshold (see Fig. 4) begins to a occur at those energies at which the WKB wave functions—which show no quantum reflection—may be increasingly trusted. At these energies where WKB is valid we may simply use the well-known WKB amplitude factor $1/\sqrt{k(x)}$, to conclude that

$$\phi_e(x_{\text{inside}})\sim \sqrt{k} \quad \text{postthreshold.} \tag{71}$$

The probability density of being found inside then behaves like k^2 at threshold (quantum reflection) and like k at postthreshold (no quantum reflection), respectively.

The probability density inside the interaction region is smaller compared to the outside by a factor of k, even when there is no quantum reflection; this is simply a kinematical effect. Classically what is unexpected is that for small enough k near threshold, the probabilities inside are *further* suppressed by a factor of k. Quantum reflection of the amplitude from the region around $|V(x)|=\epsilon$ (Sec. IX), goes hand in hand with the quantum suppression of the amplitude within this region. So finally including this k dependence of the amplitude of $\phi_e(x)$ found in Eqs. (70) and (71) we get

$$P_{e\to c}\propto k \quad \text{threshold,}$$

$$P_{e\to c}\propto \text{const} \quad \text{postthreshold.} \tag{72}$$

2. Incidence on a cluster

Since for large wavelengths only the *s* wave interacts with the cluster it is clear that the problem may be reduced in the usual manner to a one-dimensional problem again. Therefore for a unit *s-wave flux* the inelastic probabilities will behave as before as in Eqs. (72), but what is really relevant is a unit *plane-wave* flux which provides a *s*-wave flux of π/k^2. i.e. Even though the problem is one-dimensional in the radial co-ordinate, the required normalization for the incoming flux is not fixed to be a constant as before, but is now required to grow as $\sim 1/k^2$, in order to correctly account for the increasing (as $k \to 0$) range of impact parameters that all "count as" *s* wave. Thus we have simply to multiply the one-dimensional probabilities of Eqs. (72) by this factor of $1/k^2$, and conclude that the inelastic cross sections for this cluster geometry behave like

$$\sigma_{e\to c} \propto \frac{1}{k} \text{ threshold,}$$

$$\sigma_{e\to c} \propto \frac{1}{k^2} \text{ postthreshold.} \tag{73}$$

The threshold result of Eq. (73) is just the Wigner 1/v law we spoke of in Sec. XIII. But now we can say more. As the incoming wavelength λ increases, we first witness for large enough λ a quadratic dependence to the exothermic cross section ($\sigma \propto \lambda^2$). It is only at still larger wavelengths that this dependence eventually changes over to a linear one ($\sigma \propto \lambda$). This happens when the sticking yields to the quantum reflection. This energy is mostly determined by the long-range form of the potential, and has nothing to do with the bound-state energies or any other details involving the interaction potential.

XIV. CONCLUSION

We have presented a general approach to the low-energy sticking problem, in the form of *R*-matrix theory. Several supporting arguments for the nonsticking conclusion were given. Perhaps most valuable is the physical decoherence picture associated with the conclusion that there is no sticking in the zero translational energy limit.

Reviewing the observations leading up to the nonsticking conclusion, we start with the near 100% sticking in the zero translational energy limit classically (sticking probability 1). We then invoke the phenomenon of quantum reflection (Fig. 1), which keeps the incident particle far from the surface (sticking probability 0). Third, we note that quantum reflection can be overcome by resonances (Fig. 2), and since resonances are ubiquitous in a many body target, being the Feshbach states by which a particle could stick to the surface, perhaps sticking approaches 1 after all. Fourth, we suggest that decoherence (from the perspective of the incoming channel, with elastic scattering defined as coherent) ruins the resonance effect, reinstating the quantum reflection as the determining effect. Finally, then, there is no sticking, and the short answer as to why is: quantum reflection and many channel decoherence. The ultrashort explanation is simply quantum reflection, but this is dangerous and nonrigorous, as we have tried to show.

Having thus shown that the entrance channel wave function is largely unaffected by all the internal degrees of freedom we were able to predict sticking probabilities solely by consideration of the long-range forces acting on the atom. WKB proved to be a valuable tool in this context, especially since it nicely contrasts the classical behavior (of sticking) with quantum reflection. The old Wigner threshold law when viewed in this light naturally led to the discovery of certain definite postthreshold laws which are obeyed as soon as the classical behavior becomes valid at slightly higher temperatures.

ACKNOWLEDGMENTS

A.M. thanks Alex Barnett for pointing him to the references on the Casimir interactions. This work was supported by the National Science Foundation through a grant for the Institute for Theoretical Atomic and Molecular Physics at Harvard University and Smithsonian Astrophysical Observatory: National Science Foundation Award Number CHE-0073544. This work was also supported by the National Science Foundation by grants PHY-0071311 and PHY-9876927.

APPENDIX A: QUANTUM SUPPRESSION

Proposition: As $k_e \to 0$ the amplitude of $\phi(x;k_{ex})$ in the internal region $x<a$ goes to zero as $k_e \sim \sqrt{\epsilon}$.

A little thought aided by a sketch of the wave function, such as in Fig. 1, will easily convince one of the truth of this statement. Here we will spell out the argument as one might naturally think of it.

Suppose we temporarily disregard the required normalization of $\phi(x;k_x)$ of Eq. (5) and fix its initial conditions (slope and value) at some point inside the interaction region $x<a$ such that the regularity condition is ensured. Then we integrate out to $x=a$. Let us denote this unnormalized solution with a prime, as $\phi'(x;k_x)$. The point is that for k_x varying near 0, both v (the value) and s (the slope) that the solution emerges with at $x=a$, are independent of k_x and in fact the interior solution thus obtained is itself independent of k_x. This is because the local wave vector $k(x) = \sqrt{2m[\epsilon - U(x)]/\hbar^2}$ essentially stays the same function of x for all ϵ near 0. Therefore for $x>a$ $\phi'(x;k_x)$ continues onto

$$v \cos[k_x(x-a)] + \frac{s}{k_x} \sin[k_x(x-a)], \quad x>a. \tag{A1}$$

This is a phase-shifted sine wave of amplitude $\sim 1/k_x$. We must enforce the normalization of Eq. (5) and therefore get $\phi(x;k_x) \sim k_x \phi'(x;k_x)$ which is the proposition.

APPENDIX B: R MATRIX AND S MATRIX

S is found in analogy to the one-dimensional case by introducing the matrix version of the inverse logarithmic derivative at $x=a$ called $\mathbf{R}(E)$ the Wigner **R** matrix defined by

$$\vec{v} = \mathbf{R}(E)\vec{s}, \tag{B1}$$

where the components of $\vec{v}$ and $\vec{s}$ are the expansion coefficients of $\psi(x=a,u)$ and $\partial\psi(x=a,u)/\partial x$, respectively, in the $\Omega_c(u)$ basis.

1. The R matrix

Supposing $\partial\psi(x=a,u)/\partial x$ to be known, we will (like in electrostatics) use the Neumann Green's function $G_N(x,u;x',u')$ to construct $\psi(x,u)$ everywhere in the interior $x<a$. $\psi(x,u)$ satisfies the full Schrödinger equation with energy E. We need $\chi_\lambda(x,u)\lambda=1,2,\ldots$, the normalized eigenfunctions of the full Schrödinger equation in the interior $x<a$ with energies E_λ, satisfying Neumann boundary conditions $\partial\chi(x=a,u)/\partial x=0$. So

$$\left(\frac{-\hbar^2}{2m}\nabla^2+V_{\rm int}(x,u)-E\right)\psi(x,u)=0, \tag{B2}$$

$$\left(\frac{-\hbar^2}{2m}\nabla^2+V_{\rm int}(x,u)-E_\lambda\right)\chi_\lambda(x,u)=0, \tag{B3}$$

$$\left(\frac{-\hbar^2}{2m}\nabla^2+V_{\rm int}(x,u)-E\right)G_N(x,u;x',u') = \delta(x-x')\,\delta(u-u'), \tag{B4}$$

where $\nabla^2\equiv\partial^2/\partial x^2+\partial^2/\partial u^2$ and

$$\partial G_N(x=a,u;x',u')/\partial x=0 \quad\text{and}\quad \frac{\partial\chi(x=a,u)}{\partial x}=0 \tag{B5}$$

$$\Rightarrow G_N(x,u;x',u')=\sum_{\lambda=1}^{\infty}\frac{\chi_\lambda(x,u)\chi_\lambda(x',u')}{E_\lambda-E}. \tag{B6}$$

G_N is symmetric in the primed and unprimed variables. By Stokes' theorem,

$$(-\hbar^2/2m)\int_{x'<a}dx'\int_{\text{all }u'}du'(\phi_1\nabla'^2\phi_2-\phi_2\nabla'^2\phi_1) = (-\hbar^2/2m)\int_{x'=a,\text{all }u'}du'(\phi_1\nabla'_{\hat{n}}\phi_2-\phi_2\nabla'_{\hat{n}}\phi_1), \tag{B7}$$

where $\nabla'_{\hat{n}}(\cdot)\equiv\hat{x}'(\cdot)\cdot\nabla'$ with $\phi_1=\psi(x',u')$ and $\phi_2=G_N(x,u;x',u')$ gives

$$\psi(x,u)=\frac{\hbar^2}{2m}\int_{\text{all }u'}du'\,G_N(x,u;x',u')\frac{\partial\psi(x'=a,u')}{\partial x'}, \quad x<a. \tag{B8}$$

Put $x=a$ and it is deduced using Eqs. (B1), (B6), and (B8) together that

$$R_{cc'}(E)=\sum_{\lambda=1}^{\infty}\frac{\gamma_{\lambda c}\gamma_{\lambda c'}}{E_\lambda-E}, \tag{B9}$$

where $\gamma_{\lambda c}=\sqrt{\frac{\hbar^2}{2m}}\int_{\text{all }u}du\,\chi_\lambda(a,u)\Omega_c(u)$.

2. The S matrix

Now shifting attention to the outside $(x>a)$, we see that we can compute both $\nabla_{\hat{n}}\psi(a,u)$ and $\psi(a,u)$ on the surface $x=a$ using the asymptotic form of Eq. (8) which automatically gives these expanded in the $\Omega_c(u)$ basis. Writing the matrix Eq. (B1) is now simple. It is best to do it all in matrix notation, and thus be able to treat all possible independent asymptotic boundary conditions simultaneously.

Let e^{ikx}, $\sqrt{k}$, and $1/\sqrt{k}$ be diagonal matrices with diagonal elements e^{ik_cx}, $\sqrt{k_c}$, and $1/\sqrt{k_c}$. Then Eq. (B1) reads

$$\frac{e^{-ika}}{\sqrt{k}}-\frac{e^{ika}}{\sqrt{k}}\mathbf{S}=i\mathbf{R}k\left(\frac{-e^{-ika}}{\sqrt{k}}-\frac{e^{ika}}{\sqrt{k}}\mathbf{S}\right). \tag{B10}$$

Each column $c=1,\ldots,n$ of the matrix equation above is just Eq. (B1) for the solution corresponding to an incoming wave only in channel c (for $c>n$ the wave functions blow up as $x\to\infty$). Remembering that nondiagonal matrices do not commute, we solve for $\mathbf{S}$ to get

$$\mathbf{S}=e^{-ika}\sqrt{k}\,\frac{1}{1-i\mathbf{R}k}(1+i\mathbf{R}k)\frac{1}{\sqrt{k}}e^{-ika} \tag{B11}$$

which with some simple matrix manipulation yields Eq. (9) of Sec. IV. It may be shown that the open-open part of the $\mathbf{S}$ matrix—the $n\times n$ submatrix $S_{cc'}$ with $c,c'=1,2,\ldots,n$—is unitary.

APPENDIX C: $\Gamma\simeq nD$

With the large number of degrees of freedom involved and assuming thorough phase space mixing associated with the resonance we may reasonably describe the compound state wave function by a classical ensemble of points (x,p_x,u,p_u) in the combined phase space of the joint system given by the normalized distribution

$$\frac{1}{\rho_C(E)}\delta[E-H(x,p_x,u,p_u)]. \tag{C1}$$

It is understood in the above that the system is restricted to be in the region $x<a$. This makes all accessible states of energy E with $x<a$ equally likely. Then the rate of escape $\Gamma/\hbar$ through the hypersurface $x=a$ of the members of this ensemble is

$$\frac{\Gamma}{\hbar}=\frac{1}{\rho_C(E)}\int_{x=a}du\,dp_u\int_{p_x\in[0,\infty]}dp_x\frac{p_x}{m} \times\delta[E-H(x,p_x,u,p_u)]. \tag{C2}$$

p_x/m is just the velocity in phase space of a point at $x=a$ in

the $\hat{x}$ direction. At $x=a$ we have supposed no interaction. Hence the Hamiltonian separates in Eq. (C2). Therefore

$$\frac{\Gamma}{\hbar}=\frac{1}{\rho_C(E)}\int dudp_u\int_0^\infty d\left(\frac{p_x^2}{2m}\right)\times\delta\left[E-\left(\frac{p_x^2}{2m}+H^{\text{target}}(u,p_u)\right)\right] \tag{C3}$$

$$=\frac{1}{\rho_C}\int_{H^{\text{target}}(u,p_u)<E}dudp_u \tag{C4}$$

$$=\frac{1}{\rho_C}\Omega_C\simeq\frac{1}{2\pi\hbar\rho_Q}\Omega_Q=\frac{1}{2\pi\hbar}nD. \tag{C5}$$

Therefore $\Gamma/D\simeq n$. ρ_Q (ρ_C) is the quantum (classical) density of states (phase space volume) of the joint system at energy E. Ω_Q (Ω_C) is the quantum (classical) total number of states (total phase space volume) of only the target below energy E. We have used the correspondence between the classical and quantum density of states. $1/\rho_Q$ is identified with D, and the number of states of the target having energy less than E is just n, the number of open channels.

[1] J. E. Lennard-Jones *et al.*, Proc. R. Soc. London, Ser. A **156**, 6 (1936).
[2] T. W. Hijmans, J. T. M. Walraven, and G. V. Shlyapnikov, Phys. Rev. B **45**, 2561 (1992).
[3] W. Brenig, Z. Phys. B **36**, 227 (1980).
[4] D. P. Clougherty and W. Kohn, Phys. Rev. B **46**, 4921 (1992).
[5] E. R. Bittner, J. Chem. Phys. **100**, 5314 (1993).
[6] P. S. Julienne and F. H. Mies, J. Opt. Soc. Am. B **6**, 2257 (1989).
[7] P. S. Julienne, A. M. Smith, and K. Burnett, Adv. At., Mol., Opt. Phys. **30**, 141 (1992).
[8] L. D. Landau and E. M. Lifshitz, *Quantum Mechanics (Non-relativistic Theory)* (Pergamon Press, Oxford, UK, 1981).
[9] C. J. Joachain, *Quantum Collision Theory* (North-Holland, Amsterdam, 1975).
[10] G. F. Gribakin and V. V. Flambaum, Phys. Rev. A **48**, 546 (1993).
[11] R. Côte, E. J. Heller, and A. Dalgarno, Phys. Rev. A **53**, 234 (1996).
[12] I. A. Yu, J. M. Doyle, J. C. Sandberg, C. L. Cesar, D. Kleppner, and T. J. Greytak, Phys. Rev. Lett. **71**, 1589 (1993).
[13] J. M. Doyle, J. C. Sandberg, I. A. Yu, C. L. Cesar, D. Kleppner, and T. J. Greytak, Phys. Rev. Lett. **67**, 603 (1991); C. Carraro and M. W. Cole, Phys. Rev. B **45**, 12 930 (1992); T. W. Hijmans, J. T. M. Walraven, and G. V. Shlyapnikov, *ibid.* **45**, 2561 (1992).
[14] F. T. Smith, Phys. Rev. **118**, 349 (1960).
[15] A. M. Lane and R. G. Thomas, Rev. Mod. Phys. **30**, 416 (1958) (see pages following 302).
[16] T. Ericson, Phys. Rev. Lett. **5**, 430 (1960).
[17] N. Bohr and J. Wheeler, Phys. Rev. **56**, 416 (1939) (see page 436, Sec. III).
[18] G. Vidali, G. Ihm, Hye-Young Kim, and Milton Cole, Surf. Sci. Rep. **12**, 133 (1991).
[19] R. E. Grisenti, W. Schoelkopf, J. P. Toennies, G. C. Hergerfeldt, and T. Kohler, Phys. Rev. Lett. **83**, 1755 (1999).
[20] R. Cote, H. Friedrich, and J. Trost, Phys. Rev. A **56**, 1781 (1997).
[21] L. Spruch and Y. Tikochinsky, Phys. Rev. A **48**, 4213 (1997).
[22] E. A. Hinds and V. Sandoghdar, Phys. Rev. A **43**, 398 (1991) (in particular Sec. II).
[23] Ite A. Yu *et al.*, Phys. Rev. Lett. **71**, 1589 (1993).
[24] T. W. Hijmans, J. T. M. Walraven, and G. V. Shlyapniko, Phys. Rev. B **45**, 2561 (1992).
[25] E. P. Wigner, Phys. Rev. **73**, 1002 (1948).